



Publication Year	1995
Acceptance in OA	2022-10-04T14:42:46Z
Title	The bright linear type II SN 1990K
Authors	CAPPELLARO, Enrico, Danziger, I. J., DELLA VALLE, Massimo, Gouiffes, C., TURATTO, Massimo
Handle	http://hdl.handle.net/20.500.12386/32688
Journal	ASTRONOMY & ASTROPHYSICS
Volume	293

The bright linear type II SN 1990K^{*}

E. Cappellaro^{1,2}, I.J. Danziger¹, M. Della Valle^{1,3}, C. Gouiffes⁴, and M. Turatto²

¹ European Southern Observatory, Karl-Schwarzschild-Strasse 2, D-85748 Garching bei München, Germany

² Osservatorio Astronomico di Padova, vicolo dell'Osservatorio 5, I-35122 Padova, Italy

³ Dipartimento di Astronomia, Università di Padova, vicolo dell'Osservatorio 5, I-35122 Padova, Italy

⁴ DAPNIA Sap/C.E. Saclay F-91191 Gif sur Yvette Cedex, France

Received 28 February 1994 / Accepted 26 July 1994

Abstract. We obtained extensive photometric and spectroscopic observations of the Linear type II SN 1990K. The photometry suggests that the SN suffered a relatively high extinction ($A_B \simeq 2\ mag$) and was therefore very bright at maximum ($M_V^0 \leq -18.9$). However, the luminosity in the exponential tail is very similar to that of other SNI, in particular to SN 1987A, indicating that the explosion produced a similar mass of radioactive material ($M(^{56}Ni) \simeq 0.1 M_\odot$).

The spectral evolution is typical for SNI, very similar for instance to that of the SN 1987A (neglecting the fact that the latter SN showed unusually strong BaII lines). The line flux evolution of SN 1990K compared with that of other SNe and with theoretical models indicates that the envelope mass of SN 1990K was relatively low ($\sim 5 M_\odot$). Also, the envelope density is probably low (i.e. a factor 3 lower than in SN 1987A).

Two months after discovery a bump appeared in the blue side of the $H\alpha$ line which has a strong similarity to the same feature observed in SN 1987A (Bochum event) and in SN 1988A and has been related to the emergence of radioactive material into the outer hydrogen-rich envelope.

Key words: supernovae: general – supernovae: SN 1990K – galaxies: NGC 150

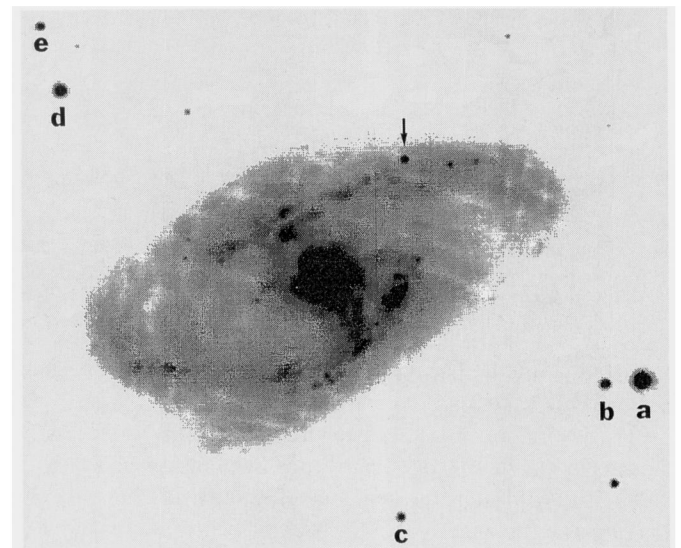


Fig. 1. SN 1990K in NGC150 and reference stars. The image is an R frame obtained at the 3.6m telescope on Oct. 26, 1990. North is up, East is left

Observations of the SN at ESO-La Silla, obtained in the framework of the ESO Key Programme dedicated to the study of SNe, started on May 30 and were terminated 16 months later. The SN 1990K belongs to the class of Bright Linear SNI. The extensive set of optical observations makes SN 1990K one of the best studied objects of this class.

1. Introduction

The SN 1990K was found by Evans (1990) on May 25.8 UT (J.D. 2448037.3) in the SBb galaxy NGC 150. It was located $18^{\circ}4'W$, $26^{\circ}6'N$ from the galaxy nucleus, superimposed on a galaxy spiral arm (Fig. 1). The absolute position was determined by McNaught & Sadler (1990) as $\alpha = 0^h31^m45^s.371$, $\delta = -28^{\circ}04'18''58$ (1950.0). Prompt spectroscopic observations indicated that the SN was of type II probably within 15–20 days from explosion (Phillips 1990).

^{*} Based on observations collected at ESO-La Silla (Chile)

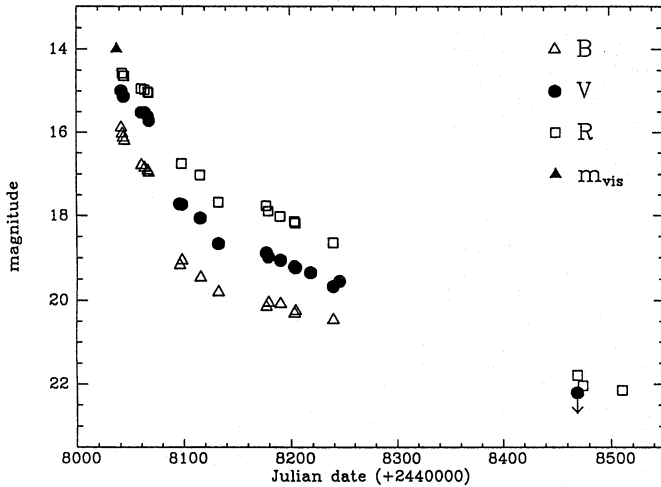
2. Observations

CCD photometric observations of SN 1990K were obtained on 23 nights using four different telescopes (Table 2).

When the nights were photometric, the frames were calibrated through observations of Landolt standard stars (Landolt 1983, 1992) and thereafter the magnitudes of a set of reference stars within the field were determined. These reference stars were used to calibrate the observations obtained on non-

Table 1. Magnitudes of the reference stars in the field of SN 1990K.

star	B	V	R
a	15.10±0.03	14.69±0.03	14.36±0.02
b	18.45±0.02	17.68±0.02	17.17±0.02
c	20.49±0.04	18.99±0.04	17.90±0.02
d	17.14±0.02	16.59±0.02	16.24±0.02
e	19.19±0.02	18.59±0.02	18.21±0.02

**Fig. 2.** B, V and R light curves of SN 1990K. The visual magnitude at discovery, from Evans (1990), has an uncertainty of ~ 0.5 mag

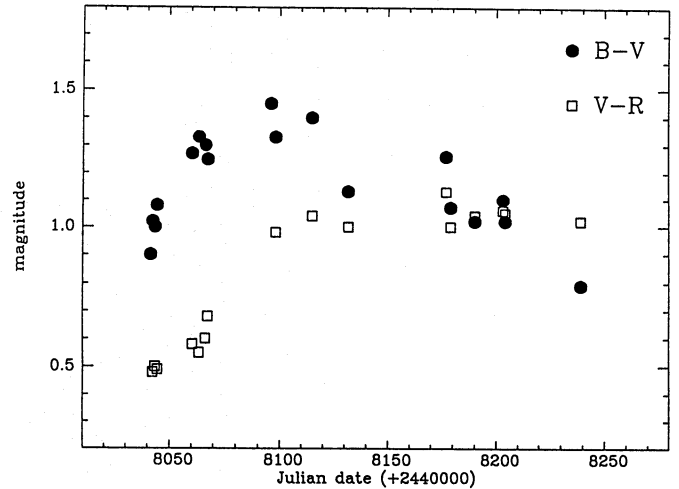
photometric nights. The magnitudes of the reference stars, identified in Fig. 1, are reported in Table 1.

The SN magnitudes have been measured using the Romafot package in MIDAS. After measuring the point spread function (PSF) from field stars, the program allows the simultaneous fitting of the target object and of the background, the latter approximated by a tilted plane. The major problem in SN photometry is the subtraction of the complex galaxy background, especially when the SN fades. In this respect the PSF fitting gives more reliable results than aperture photometry (cf. Turatto et al. 1993).

Results are reported in Table 2 where in cols. 1 and 2 are the date and J.D. of observations, in cols. 3-6 the B, V, R and I magnitudes along with an estimate of the internal errors, in col. 7 the seeing (FWHM) and in col. 8 the equipment used.

The light curve of SN 1990K in B, V and R bands is shown in Fig. 2.

The rise in brightness has not been observed, hence the epoch of maximum is not known. In the following as reference we use the date of discovery (J.D. = 2448037.3). During the first 100 days after discovery, the light curves show a steep, almost linear, decline. A linear fit of the data gives $\beta_{100}^B = 4.7 \pm 0.3$, $\beta_{100}^V = 4.4 \pm 0.3$ and $\beta_{100}^R = 3.6 \pm 0.2 \text{ mag}(100d)^{-1}$, which are typical of *Linear* SNII (Patat et al. 1993b). We note that the observations obtained 20-30 days after discovery show the presence of a shoulder in the light curves which means that they are not truly linear. This is not uncommon in *Linear* SNII light curves, e.g. SNe 1970G and 1979C (Patat et al. 1993a).

**Fig. 3.** B-V and V-R color curves of SN 1990K

After this first 100 day phase the luminosity decline settles down at a significantly smaller rate. In the phase range 100-210 days the decline rates are $\gamma_B = 0.6 \pm 0.1$, $\gamma_V = 1.0 \pm 0.1$ and $\gamma_R = 1.3 \pm 0.2 \text{ mag}(100d)^{-1}$, which are similar to the average for SNII (Turatto et al. 1990). The observations were then interrupted because of the seasonal limitation. The SN was recovered, albeit very faint, over 200 days later, about 15 months after discovery. The photometric errors at these late stages are relatively large but the measurements are consistent with a constant decline rate: in the phase range 200-470 the decline rates are $\gamma_R = 1.3 \pm 0.1$ and $\gamma_V \geq 1.1 \pm 0.1$ (the late V measurement is an upper limit).

Also the color evolution of SN 1990K (Fig. 3) is typical of *Linear* SNII (Patat et al. 1993b). The B-V color exhibits a rapid evolution from blue to red (rate $\beta_{B-V} = 1.3 \text{ mag}(100d)^{-1}$) until a maximum is reached at about 50 days. From here on the color slowly becomes bluer ($\beta_{B-V} = -0.4 \text{ mag}(100d)^{-1}$). However, at all phases the color of SN 1990K is significantly redder than that of other SNII *Linear*. Indeed the color curves of well observed SNII *Linear* can be matched by adopting a color excess $E(B-V) = 0.5 \pm 0.1$. Also the fit is improved if we assume that the SN was discovered a couple of weeks past maximum (Fig. 4).

Adopting a standard reddening law this implies an absorption $A_B = 2.0 \pm 0.4$ mag. Because the galactic extinction in the direction of NGC 150 is only $A_B = 0.07$ (Burstein & Heiles 1978), the large extinction suffered by SN 1990K must occur in the parent galaxy.

Because SN 1990K was not observed at maximum we can give only an upper limit to the maximum SN brightness: $V \leq 14.0 \pm 0.5$. Adopting for the parent galaxy NGC 150 a distance modulus $\mu = 31.42$ (Tully 1988) and for the extinction $A_V = 1.5 \pm 0.3$, we derive an absolute magnitude at maximum $M_V^0 \leq -18.9 \pm 0.6$. This is expected to be very similar to the absolute B magnitude since at maximum $(B-V)_0 \approx 0$.

The absolute magnitude of SN 1990K is then more than 2 mag brighter than the regular SNII ($\langle M_B \rangle = -16.5 \pm 0.6$).

Table 2. Photometry of SN 1990K

Date	J.D. +2440000	B	V	R	I	seeing (arcsec)	Telescope
30/5/90	8041.41	15.89±0.05	14.99±0.03			3.2	3.6m+EFOSC
31/5/90	8042.39	16.03±0.02	15.05±0.02	14.57±0.02		1.3	NTT+EFOSC2
01/6/90	8043.39	16.13±0.03	15.13±0.03	14.63±0.03		1.7	NTT+EFOSC2
02/6/90	8044.42	16.21±0.05	15.13±0.04	14.64±0.04		1.7	NTT+EFOSC2
18/6/90	8060.40	16.79±0.02	15.52±0.02	14.94±0.02		1.6	Danish 1.5m
21/6/90	8063.42	16.85±0.02	15.52±0.02	14.97±0.02		1.1	Danish 1.5m
24/6/90	8066.42	16.92±0.04	15.62±0.03	15.02±0.03	14.69±0.06	2.1	Danish 1.5m
25/6/90	8067.42	16.97±0.02	15.72±0.03	15.04±0.02	14.84±0.02	1.1	Danish 1.5m
24/7/90	8096.21	19.17±0.03	17.72±0.02			1.4	NTT+EFOSC2
26/7/90	8098.32	19.06±0.05	17.73±0.02	16.75±0.05		1.3	3.6m+EFOSC
12/8/90	8115.36	19.46±0.04	18.06±0.03	17.02±0.03		0.9	Danish 1.5m
28/9/90	8132.12	19.80±0.04	18.67±0.03	17.67±0.02		1.1	3.6m+EFOSC
13/10/90	8177.23	20.15±0.05	18.89±0.04	17.76±0.04		1.0	Danish 1.5m
15/10/90	8179.23	20.05±0.05	18.98±0.04	17.89±0.04		1.1	3.6m+EFOSC
26/10/90	8190.22	20.08±0.10	19.06±0.03	18.02±0.02		1.3	3.6m+EFOSC
08/11/90	8203.23	20.31±0.25	19.21±0.10	18.14±0.10		2.3	MPI 2.2m
09/11/90	8204.20	20.25±0.15	19.23±0.07	18.18±0.06		1.7	3.6m+EFOSC
23/11/90	8218.07		19.35±0.10			1.2	3.6m+EFOSC
14/12/90	8239.11	20.46±0.12	19.67±0.05	18.65±0.05		2.0	Danish 1.5m
20/12/90	8245.08		19.55±0.04			1.3	3.6m+EFOSC
01/08/91	8469.24		≤22.2	21.79±0.20		1.1	MPI 2.2m
06/08/91	8474.30			22.04±0.25		1.6	3.6m+EFOSC
11/09/91	8510.28			22.15±0.30		1.4	3.6m+EFOSC

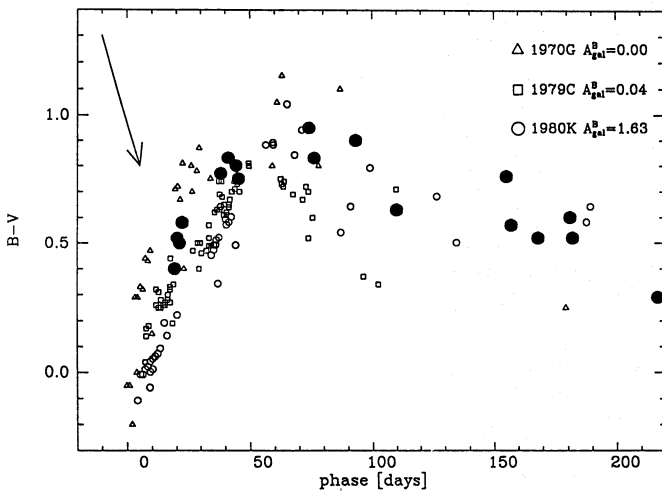


Fig. 4. Comparison of the B-V color curve of SN 1990K with those of well studied Linear SNIIs. The latter have been corrected only for galactic extinction. The arrow indicates the shift applied to the observed data of SN 1990K to best fit the average color curve of SNIIs. We conclude that SN 1990K suffered a color excess $E(B-V)=0.5 \pm 0.1$ mag and, most likely, was discovered about 15 days after maximum

and indicates this SN is a member of the rare class of Bright Linear SNIIs, having $\langle M_B \rangle = -18.9 \pm 0.6$ (cf. Patat et al. 1993b).

Although SNIIs at early stages can exhibit very different light curves, with a range of 5 mag in absolute magnitude at maximum light, at late phases most of them seem to converge to

a similar absolute magnitude (Turatto et al. 1990; Patat et al. 1993b). Once corrected for the adopted interstellar extinction SN 1990K conforms to this finding. This is shown in Fig. 5 where we compare the V absolute light curve of SN 1990K with that of the linear SN 1979C and of SN 1987A. Whereas at discovery SN 1990K and SN 1979C were 5 magnitude brighter than SN 1987A, 150 days later all SNe converge to very similar luminosities. This conclusion does not strongly depend on the adopted value of H_0 assumed in determining distances to all these objects.

3. Spectroscopy

3.1. Spectral evolution

The log of the spectroscopic observations is reported in Table 3. Each spectrum has been wavelength calibrated using He-Ne comparison lamp and flux calibrated by comparison with observations of standard stars (Stone 1977; Stone & Baldwin 1983, 1984; Massey et al. 1988, 1990).

The absolute flux calibration of the spectra has been verified against the B, V and R photometry. The agreement is generally quite good but for the 1990 May 31 spectrum where the B-V color derived from the spectrum was found 0.5 mag larger than the photometric measurement. The spectrum has been corrected accordingly but the flux calibration in the extreme blue remains uncertain.

In Table 3 are indicated the date and J.D. of observations (cols. 1-2), the phase relative to discovery (col.3), the equipment used (col.5), the exposure time (col. 6), the spectral range (col.

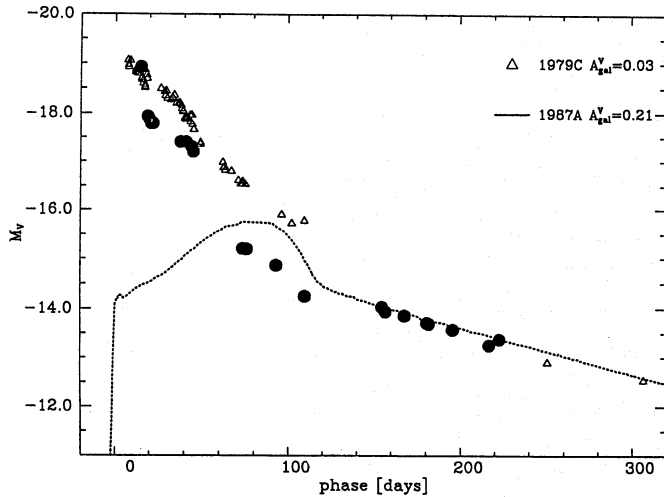


Fig. 5. Comparison of the V absolute light curve of SN 1990K with that of SN 1979C and SN 1987A. For the SN 1990K an extinction $A_V = 1.5$ mag is assumed. The magnitudes of the other two SNe are corrected only for galactic extinction. Again, it is assumed that the SN have been discovered 15 days after maximum

7) and the resolution derived from the average FWHM of night-sky lines (col. 8). In several cases, when a good wavelength coverage and resolution were obtained using different grisms, the cumulative exposure times are indicated.

The SN is projected on a spiral arm, close to many HII regions which show up in the long slit spectra with narrow emission lines adjacent to the SN spectrum. The heliocentric radial velocity at the location of the SN has been derived by taking the average of the measurements of the narrow emission lines in all the spectra. The resulting heliocentric velocity is $1450 \pm 20 \text{ km s}^{-1}$. The difference with the value reported in Tully (1988), $v = 1593 \text{ km s}^{-1}$, is probably due to the rotational velocity of the parent galaxy.

In the spectra of higher S/N we note a narrow absorption corresponding to the NaID doublet at the redshift of the parent galaxy. The equivalent width of this feature, $\sim 1 \text{ \AA}$, confirms that the SN suffered a significant reddening. According to the empirical relation derived by Barbon et al. (1990) this would imply an interstellar reddening $E(B - V) \sim 0.25$ mag, which corresponds to half the value derived from the B-V color curve. However the relation between extinction and EW(NaID) is not well determined. The same relation deduced from the measurements of Cohen (1975) would indicate an extinction equal to that measured from the photometry, $E(B-V) \sim 0.5$ mag, which will be adopted in the following.

The spectral evolution of the SN is illustrated in Fig. 6 where nearly contemporaneous spectra have been averaged to increase the signal to noise and/or to extend the wavelength coverage.

As is typical for SNe, the evolution is initially very rapid. At early epochs the bulk of the flux is emitted in the continuum. When corrected for the large extinction the continuum appears relatively blue (black body temperature $\sim 7000^\circ \text{ K}$). Major features in the spectra have pronounced P-Cygni profiles and, as

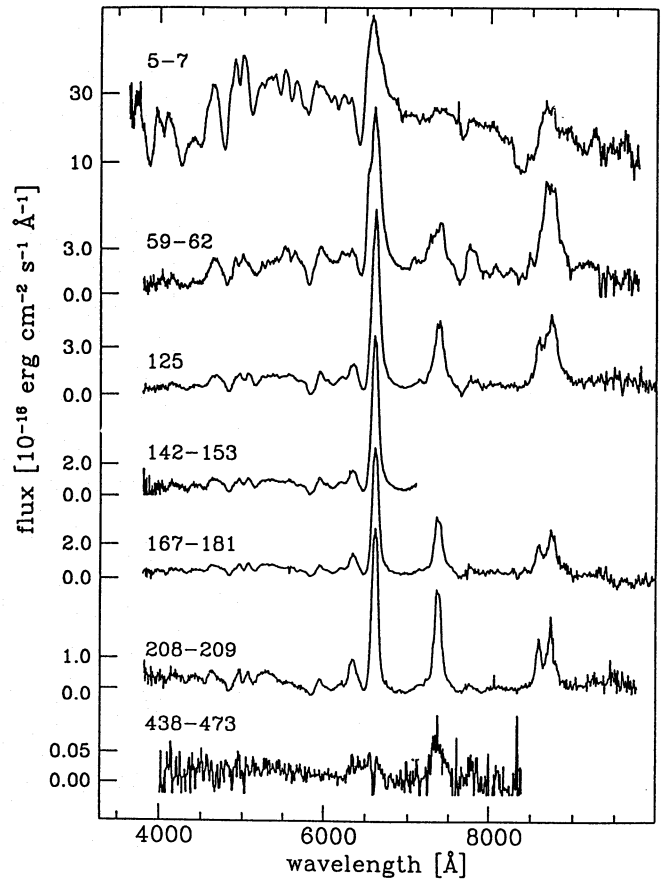


Fig. 6. Spectral evolution of SN 1990K. Spectra taken at similar epochs have been averaged to improve the S/N and/or the wavelength coverage. In these cases, the phase range of the averaged spectra is indicated. In the last spectrum a narrow absorption at 6600 \AA is due to over-subtraction of the nearby HII region. Wavelength is in the observer rest frame and flux is not corrected for extinction

indicated in the next section, they are mostly due to permitted transitions of light elements. In two months the continuum becomes significantly fainter and redder, forbidden transitions emerge and lines of heavy elements, in particular Fe, appear. From then on the general appearance of the spectrum remains unchanged but with forbidden lines becoming increasingly important as the density of the line emitting region decreases.

An indicator of this evolution is the relative ratio of the [CaII]/CaII lines. The red part of the early spectrum is dominated by the CaII IR triplet. Two months later the [CaII] 7291-7324 \AA feature first appears and progressively grows in strength, until 6 months after discovery, it becomes stronger than the CaII IR lines. From here on it competes in intensity with $H\alpha$ until, 15 months after discovery, the [CaII] 7291-7324 \AA doublet is the dominant feature in the optical spectrum. At this epoch the broad feature in the range 6250-6750 \AA is a blend of $H\alpha$ and [OI] 6300-6364 \AA lines having roughly the same strength.

It is difficult to perform a detailed comparison of the spectral evolution of SN 1990K with that of other Linear SNII since very few good S/N spectra have been published so far. Some

Table 3. Spectroscopic observations of SN 1990K

date	J.D. +2440000	phase* (days)	telescope & instrument	exp. time (min)	spectral range Å	resolution Å
30/05/90	8041.94	+5	3.6m+EFOSC	10	5800-9600	23
31/05/90	8042.91	+6	NTT+EFOSC2	20	3600-7000	23
01/06/90	8043.90	+7	NTT+EFOSC2	20	6000-8200	18
24/07/90	8096.50	+59	NTT+EFOSC2	50	3600-7000	7
26/07/90	8098.83	+62	3.6m+EFOSC	35	3800-9500	16
10/08/90	8113.80	+77	1.5m+B&C	30	4000-6800	8
28/09/90	8162.71	+125	3.6m+EFOSC	120	3800-9500	21
15/10/90	8179.75	+142	3.6m+EFOSC	30	3800-7000	14
18/10/90	8182.61	+145	MPI 2.2m+B&C	80	4000-6900	6
26/10/90	8190.75	+153	3.6m+EFOSC	30	3800-7000	15
09/11/90	8204.75	+167	3.6m+EFOSC	60	4000-10000	21
23/11/90	8218.58	+181	3.6m+EFOSC	60	3900-10000	16
20/12/90	8245.62	+208	3.6m+EFOSC	60	3600-7000	16
21/12/90	8246.54	+209	3.6m+EFOSC	50	5800-9600	18
06/08/91	8474.81	+438	3.6m+EFOSC	120	4000-8500	18
12/09/91	8510.77	+473	3.6m+EFOSC	90	4000-7000	18

* from discovery

general remarks can, however, be made in particular by comparison with the observations of the SNe 1979C (Branch et al. 1981; Barbon et al. 1982a) and 1980K (Barbon et al. 1982b; Uomoto & Kirshner 1986). The comparison with SN 1987A is also very interesting because of the superb observational and theoretical material available for this SN, and because, in terms of the photometric classification, the peculiar light curve and faint absolute magnitude SN1987A lies at the opposite extreme with respect to SN 1990K.

In the first 2/3 weeks the spectrum of a linear SNII is almost featureless, showing only a very blue continuum. At these phases the $H\alpha$ emission is very faint, or absent. It took a month for SNe 1979C and 1980K to develop an $H\alpha$ emission similar to that of SN 1990K only few days after discovery ($EW \sim -180 \text{ \AA}$). Indeed, this may also indicate that SN 1990K was discovered some time after maximum (cf. Sect. 2), but note that SNe 1979C and 1980K, unlike SN 1990K, never developed strong P-Cygni troughs. The $H\alpha$ P-Cygni absorption of SN 1987A is much deeper, but it may include a contribution from BaII (6497 Å) which is unusually strong in SN 1987A (cf. Sec. 3.3).

No significant difference can be found with the spectra of other SNII at phases later than 2 months, with the exception of the spectrum obtained at 438 days. Even if at this phase the S/N is poor it appears that in SN 1990K the [CaII] doublet is significantly stronger than $H\alpha$, which does not occur in other SNII.

The expansion velocity of the line emitting region can be traced measuring the FWHM of the $H\alpha$ line (Fig. 7). Neglecting the peculiar behaviour of SN 1979C, which always showed a very high expansion velocity, the other three SNe show a very similar kinematical pattern.

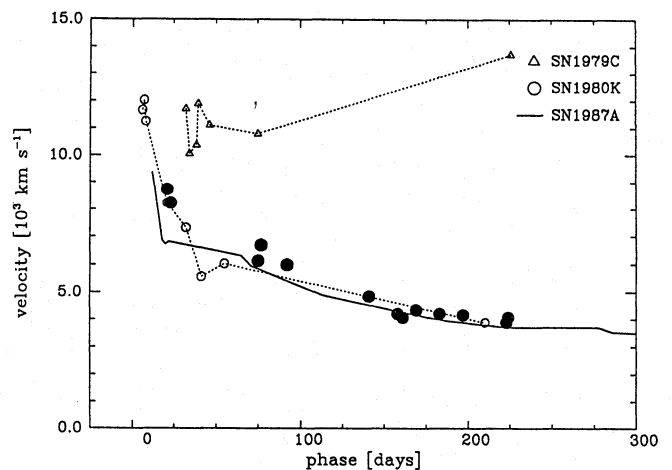


Fig. 7. Ejecta expansion velocity of SN 1990K from the FWHM of the $H\alpha$ emission (filled circle) compared with the same data for SN 1979C, SN 1980K and SN 1987A

3.2. Profile of the $H\alpha$ emission

The evolution of the $H\alpha$ profile in the spectra of SN 1990K is shown in Fig. 8. In the early phase the line is produced in the outer, high velocity, material and is therefore very broad. With time the photosphere and the line emitting region recede in mass coordinates, and the line becomes narrower. As expected from a theoretical model, at the beginning the peak of the emission of this strong line is blue-shifted with respect to the rest wavelength (Jeffery & Branch 1990). With time the peak moves redwards and starting 4 months after maximum it appears red-shifted by about 10 \AA compared with the rest wavelength (cf. 3.4). The line is symmetric, with an almost gaussian profile except in the very early spectrum, where the P-Cygni absorption is strong and in the spectra obtained 2 months after discovery where a bump ap-

pears on the blue wing. In the galaxy rest frame this feature has a peak at 6500 Å. This is especially interesting because a similar feature was noted in other SNII, in particular in SN 1987A (Bochum event, Hanuschik 1988, Phillips & Heathcote 1989) and SN 1988A (Turatto et al. 1993). In all these SNe the blue satellite emission occurs at a similar phase, i.e. between 1 to 3 months after maximum, and at about the same wavelength. One possible explanation of this feature is the lack of $H\alpha$ absorption in a region of the envelope of intermediate velocity, that is 2000 – 3000 $km\ s^{-1}$. In a model developed by Chugai (1991a) this is achieved by assuming that, as a consequence of the deep recombination of hydrogen at this phase, clumps of radioactive material emerge above the photosphere. Because of the low penetrating power of the exciting radiation in the relatively dense regions, the filling factor of excited hydrogen is small and therefore the screening of the photosphere by the $H\alpha$ transition is small. The reduced absorption causes the apparent emission bump on the blue wing of the $H\alpha$ profile. If the interpretation of the blue bump on $H\alpha$ is correct, the similarity of the event in three different SNII, 1990K 1987A and 1988A, suggests that the inner regions are not very different, at least with regard to the clumpiness of the radioactive material penetrating outwards and to the density structure. We recall that the three SNe had different light curves: that of SN 1990K was linear, whereas that of SN1988A was plateau and that of SN 1987A was “peculiar”. The differences in the early light curve are explained with different structures of the precursor atmosphere at the time of explosion but the similar occurrence of the blue satellite emission may indicate that the inner regions are instead quite similar.

3.3. Line identifications near maximum

By merging the first three spectra of Table 3 we obtained a good S/N spectra of the near maximum phase extending over the complete optical region. In Fig. 9 this spectrum is compared with a spectrum of SN 1987A at day 18. Neglecting the shape of the continuum, which is bluer in SN 1990K, the two spectra show a general resemblance but with a few noticeable differences. Because much work have been done on the line identification of SN 1987A (e.g. Williams 1987; Mazzali et al. 1992), this comparison is very helpful for the line identification in SN 1990K.

The most obvious features are the Balmer lines of HI that can be seen up to He. The absorption near 5750 Å appears to be a blend and is broader than the analogous feature in SN 1987A where it is attributed to the NaID doublet. In SN 1990K HeI (5876 Å) at relatively high velocity ($\sim 8000\ km\ s^{-1}$) probably contributes to this feature. The CaII lines, both the near-infrared triplet (8498-8542-8662 Å) and the H and K lines, are very strong. The average expansion velocity of the photosphere, derived from the minimum of the P-Cygni absorption of these lines (excluding the very strong $H\alpha$ and HeII) is $v = 7000\ km\ s^{-1}$.

BaII lines in SN 1990K are much fainter than in SN 1987A (see in particular the 6142 Å line), whereas ScII lines (from another s-process element) have about the same strength. The BaII lines were unusually strong in SN 1987A compared with

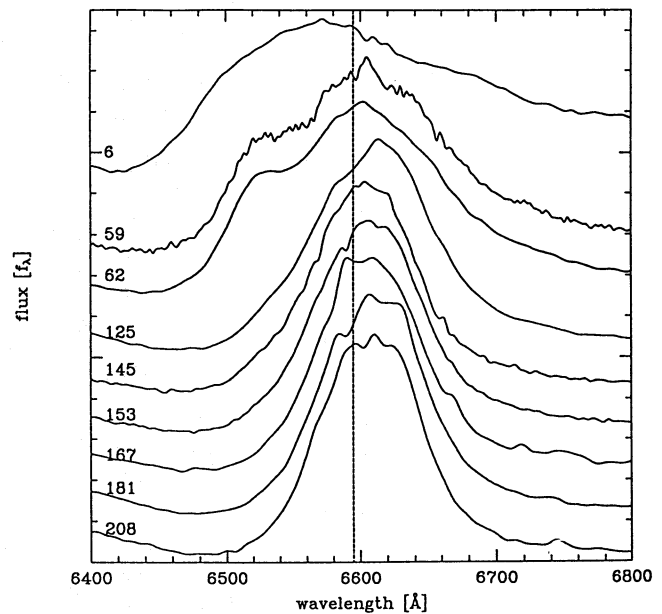


Fig. 8. Evolution of the profile of the $H\alpha$ line in SN 1990K. The dashed line marks the position of the $H\alpha$ transition in the galaxy rest frame. In two spectra, namely at 59d and 62d, a bump is present, measured at about 6510 Å, on the blue side of the emission feature. The last of it is conceivably present on day 125 at a much lower blueshift

other SNII, e.g. SN 1988A (Turatto et al. 1993) or SN 1990E (Schmidt et al. 1993). This may be partially related to the low ionization temperature of SN 1987A. Also, for both SN 1987A and SN 1990K, the expansion velocity derived from the BaII 6142 Å line is significantly smaller than the average for the other lines ($v = 5000\ km\ s^{-1}$). This was also noted in SN 1988A and attributed to contamination by FeII 6149 Å and/or by redshifted scattered photons from NaID (Turatto et al. 1993).

The line measured at 4940 Å is probably due to ScII 5031 Å (Mazzali et al. 1992). This is of interest because this unblended line is often identified with FeII 5018 Å (multiplet 42) and used to estimate the expansion velocity of SNII photosphere. If the line is instead due to ScII the expansion velocity would be underestimated by $\sim 800\ km\ s^{-1}$. Indeed we find that the identification with ScII gives an excellent agreement with the expansion velocity derived from other lines. On the other hand, at later phases, because of the simultaneous presence of the other strong lines of the same multiplet, the FeII 5018 line is the more likely identification for the same feature (see next section).

Finally, we propose to identify the absorption measured at $\sim 7660\ Å$ with OI multiplet 1 (7774 Å). This line is heavily contaminated by telluric absorption which is often not corrected for in SN spectra. However, it was already identified in the spectra of SNe 1987A (Mazzali et al. 1992) and 1990E (Benetti et al. 1993). A contribution of multiplet 4 of OI (8446 Å) to the the CaII IR feature is also possible.

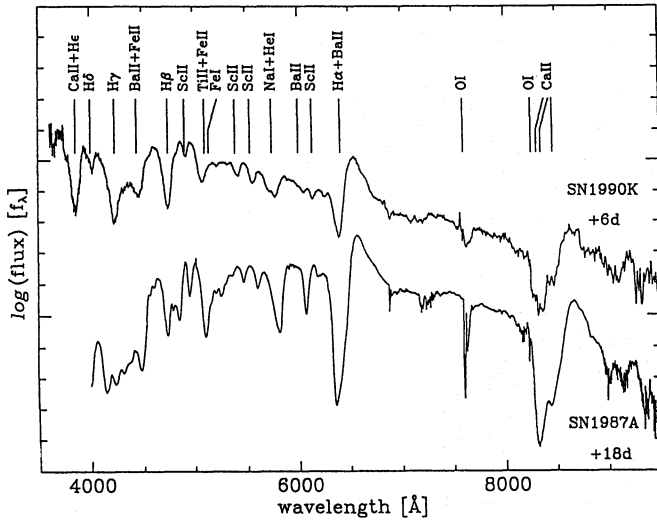


Fig. 9. Comparison on the near maximum spectrum of SN 1990K with that of SN 1987A at 18 days (ESO data set). The absorption line identifications are indicated adopting an expansion velocity of 7000 km s^{-1} . The two spectra are corrected to the galaxy rest frame and have been corrected for extinction

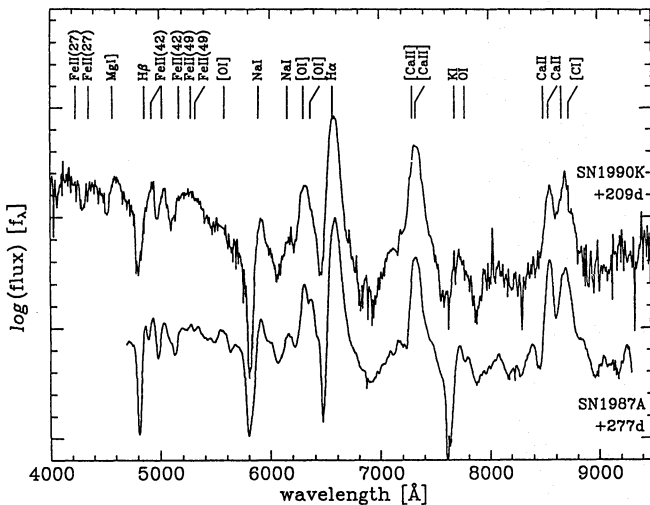


Fig. 10. Comparison between the late time spectra of SN 1990K (+210d) and SN 1987A (277d). Line identifications are indicated. The spectra are corrected to the galaxy rest frame and have been corrected for extinction

3.4. Line identifications at nebular phases

The last good S/N spectrum of SN 1990K was obtained 210 days after maximum. Again, the spectrum appears very similar to that of SN 1987A at the same phase (Fig. 10) and the same lines can be identified (cf. Phillips & Williams 1991; Danziger et al. 1991; Spyromilio et al. 1991)

The peaks of the emission lines appear red-shifted compared with the narrow lines of the adjacent HII region by $600\text{--}700 \text{ km s}^{-1}$, and this seems too large to be explained by a motion of the SN relative to the neighbour HII regions. A similar effect was also observed in SN 1987A where the centroid of emissions

Table 4. Emission line fluxes of SN 1990K 209 days after discovery

λ_0	ion	λ_{lab}	flux*
4180:	FeII (27)	4233	
4400:	FeII (27)	4352	
4604	MgI]	4571	28
4926	H β +FeII (42)	4861,4923	12
5036	FeII (42)	5018	13
5163-5393	FeII (42+49)	5169,5316-5362	36
5554:	[OI]	5577	5:
5918	NaI	5892	13
6166	NaI	6157	4
6314	[OI]	6300-6364	37
6575	H α	6563	155
7326	[CaII]	7291-7324	93
7724	KI+OI	7681,7774	6
8550-8688	CaII	8498-8542-8662	60
8743:	[CI]	8727	7:

* corrected for extinction, in unit of $10^{-15} \text{ erg cm}^{-2} \text{ s}^{-1}$

lines is displaced by $300\text{--}500 \text{ km s}^{-1}$ compared with the SN rest frame and the line profiles exhibit an extended red wing. This effect was alternatively attributed to a major anisotropy in the explosion (Spyromilio et al. 1990) or to the effect of electron scattering in the homologously expanding ejecta (Witterborn et al. 1989). Since asymmetries are not expected to appear in the same way in different SNe, the effect of Thompson scattering seems a more likely explanation.

The spectrum is dominated by H α , [CaII] 7291-7324 Å and the CaII infrared triplet. The doublets of [OI] 6300-6364 Å and the NaID 5890-96Å are also relatively strong. The latter continues to have a strong P-Cygni absorption which indicates a significant optical depth (this occurred also in SN 1987A up to ~ 2 years past maximum). The expansion velocity corresponding to the minimum of the NaID absorption is $\sim 4000 \text{ km s}^{-1}$, similar to that of SN 1987A. The 6141-6161 Å doublet of NaI may also be present. This has been attributed to a non-thermal pumping mechanism by Lucy, Danziger & Gouiffes (1991). Most of the lines shortward of 5500 Å are due to permitted FeII transitions, in particular multiplets 42, 49 and 38. MgI] 4471 Å is also present probably blended with FeII lines of multiplet 27. [FeII] emission lines, crowding the spectra of SNII 400-500 days after explosion, e.g. SN 1987A (Phillips & Williams 1991) or SN 1988A (Turatto et al. 1993), have not yet emerged. On the red side of the spectrum, KI 7681 Å and OI 7774 Å are probably contributing to the emission centered at 7730 Å (Benetti et al. 1993), whereas the hump on the red side of the CaII infrared triplet is more likely due to [CI] 8727 (Phillips & Williams 1991).

The observed positions, ion identifications and extinction corrected fluxes of the lines identified in the late time spectrum are reported in Table 4.

3.5. Lines fluxes

The evolution of the flux in the H α emission of SN 1990K is plotted in Fig. 11 and compared with the same data for SNe

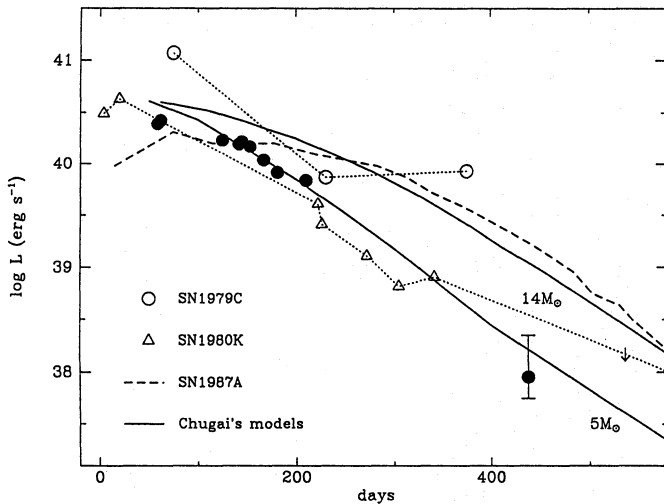


Fig. 11. Evolution of the luminosity of $H\alpha$ for SN 1990K (filled circle) compared with the same data for SN 1979C, SN 1980K and SN 1987A. Also reported are the Chugai's 5 and 14 M_{\odot} models (Chugai 1991)

1979C, 1980K and 1987A. The SNe 1990K, 1980K and 1987A show a similar $H\alpha$ flux up to 150 days, then SN 1990K and SN 1980K decline faster than SN 1987A. Again SN 1979C appears peculiar, being always significantly brighter than the others. These observations are compared with the simple model developed by Chugai (1988, 1991b) in which the late $H\alpha$ emission of SNII is energized by the radioactive decay of ^{56}Co in ^{56}Fe . Once the energy of the explosion and the mass of ^{56}Ni are fixed, the emerging flux is very sensitive to the mass of the envelope. It seems that the observations of SN 1990K (and also of SN 1980K at least up to one year after explosion) are very well fitted by a model constructed with the same Ni mass ($0.075 M_{\odot}$) and explosion energy (10^{51} erg) as SN 1987A but with an envelope mass a factor three smaller, i.e. $5 M_{\odot}$.

With the same basic assumption, i.e. input energy by radioactive decay, but with more detailed calculations, Fransson & Chevalier (1987, 1989) have also modelled the late emission of SNe. In particular they calculated the expected late emission from different progenitor models of SN 1987A. Because of the different composition and density structure one can discriminate between progenitors on the basis of the relative emission line strengths. In particular the ratio of the forbidden emission of $[\text{OI}]/[\text{CaII}]$, which has a weak dependence on temperature and density of the emitting region and therefore is expected to be rather constant with time (Fransson & Chevalier 1989), increases with the ZAMS mass of the progenitor. The evolution of the $[\text{OI}]/[\text{CaII}]$ ratio for SNe 1990K and SN 1987A is reported in Fig. 12. As expected the ratio is quite constant and, somewhat surprisingly, is very similar in the two SNe, indicating that the relative abundance of the two elements is also similar.

On the other hand, the ratio of permitted to forbidden lines of CaII, decreases with time with a similar slope in the two SNe but, at any given time, it is significantly smaller in SN 1990K, by about 0.5 dex (Fig. 12). According to Fransson & Chevalier

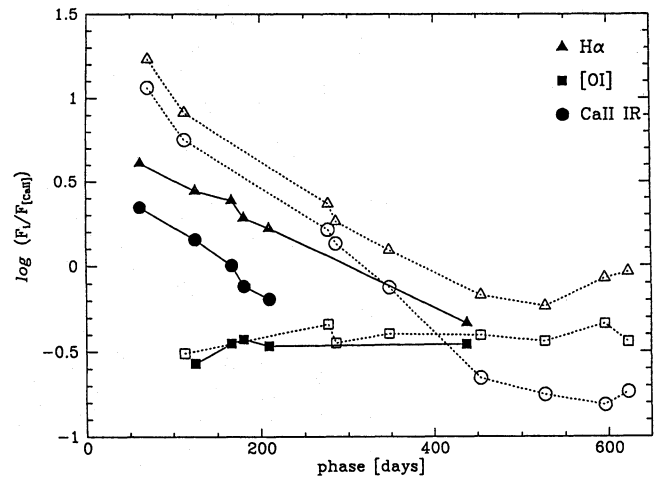


Fig. 12. Evolution of the emission of $H\alpha$, CaII infrared triplet and $[\text{OI}]$ 6300-6364 Å relative to $[\text{CaII}]$ 7291-7324 Å for SN 1990K (filled symbols) and comparison with the same data for SN 1987A (open symbols)

(1989) this can be explained if, at similar phase, the envelope density in SN 1990K is a factor 5 smaller than in SN 1987A.

4. Discussion

The photometric classification of SNII in *plateau* and *linear* was introduced by Barbon et al. (1979) on the basis of the morphological appearance of the light curves. At that time all SNII were thought to originate in the explosion of massive red supergiants via core collapse. The possible continuous sequence from the linear SN 1959D to the extended plateau SN 1969L was attributed to the occurrence of the same kind of explosion in progenitors of increasing envelope mass.

Later, Young & Branch (1989) stressed the very close match between the absolute V light curve of the linear SNII 1979C with that of the Ia SN 1972E. Also, they pointed out that, although the shapes of the light curves are similar, SNII linear are not an homogeneous class. For instance SN 1979C was, at maximum, 2-3 mag brighter than a *normal* linear SNII. SN 1979C was thereafter suggested as a prototype of a different class of SNII called bright-linear (IIB-L) (Patat et al. 1993b).

From this evidence Young & Branch (1989) proposed a different scenario in which IIL (or possibly only IIB-L) have a progenitor and explosion mechanism more similar to SNIa, rather than to IIP. Both IIL and Ia are thought to result from the deflagration of C-O degenerate core of relatively low mass stars ($\leq 8 M_{\odot}$), the only difference being that in IIL a small hydrogen envelope is left at the time of explosion, whereas this has completely vanished in Ia. This explosion is expected to produce a large amount of ^{56}Ni ($\sim 0.6 M_{\odot}$) compared to normal core collapse and therefore result in a very bright late luminosity. Moreover, the late time spectra of this C-O degenerate-core IIL should be very similar to that of Ia, i.e. dominated by FeII and FeIII emission lines and faint (if any) $H\alpha$ (Branch et al. 1991). Both these expectations are not supported by the observations.

Another scenario has been proposed by Swartz et al. (1991) in which an intermediate mass star ($8-10 M_{\odot}$) undergoes an electron-capture induced core collapse. The interest of this new scenario lies in the fact that it reproduces the basic features of the linear light curves still retaining a significant envelope mass ($\sim 3 M_{\odot}$). Also, because a small amount of ^{56}Ni is produced ($\sim 0.1 M_{\odot}$), this model is able to reproduce the observed exponential tail. However the very high maximum luminosity of IIB-L is not accounted for. To explain SNIIB-L they also suggest a carbon deflagration model.

Alternatively, according to Bartunov & Blinnikov (1992), the bright maximum of IIB-L may be explained, in a standard core collapse model, by the reprocessing of UV photons in the shell created from the presupernova superwind. An interesting feature of their model is that it has a very rapid rise to maximum (only five days from explosion). Since IIL has never been observed in the rising branch of the light curve it is likely that this is very rapid.

In favour of this last scenario we note that the two bright IIL SNe 1979C and 1980K were both detected as strong radio sources, whereas normal SNII have never been detected, with the exception of SN 1987A which, though intrinsically faint in the radio, could be detected because it was close (Weiler et al. 1991a). The radio emission of radio-loud SNe is attributed to the interaction of the SN ejecta with a dense presupernova wind. Estimates range from $M_{wind} \geq 0.34 M_{\odot}$ in SN 1980K (Weiler et al. 1992) to $M_{wind} \geq 1.3 M_{\odot}$ in SN 1979C (Weiler et al. 1991b). Based on stellar evolution models the latter implies a progenitor mass for SN 1979C $M_{ZAMS} \geq 13 M_{\odot}$ (Weiler et al. 1991b) which is in good agreement with the Bartunov & Blinnikov (1992) scenario. Chugai (1993) for SN 1986J and Chugai & Danziger (1994) for SN 1988Z have shown that these 2 SNe are among the most extreme examples of ejecta-wind interaction, giving rise to, among other things, strong radio emission. However a progenitor mass of $\sim 8 M_{\odot}$ for SN 1988Z is indicated from their work.

Finally, we note that both SN 1979C (Fesen & Matonick 1993) and SN 1980K (Fesen & Becker 1990) have been recovered, at optical wavelengths, several years after the explosion. The measured flux at these phases is much stronger than that expected from the extrapolation of the radioactive decline rate exhibited in the first two years after the explosion. Again, the source of the energy is possibly related to the interaction of the expanding SN ejecta with dense circumstellar matter (Fesen & Matonick 1993).

We review the observations of SN 1990K in the light of the different scenarios.

The spectrum of SN 1990K was, at all phases, very similar to that of SN 1987A. In particular the ratio of CaII to OI forbidden lines is exactly the same in the two SNe. In the models of Fransson & Chevalier (1987) this ratio depends on the ZAMS mass of the progenitor which, therefore, should not be very different in the two cases. We note that preferred models of SN 1987A have an initial mass in the range $15-20 M_{\odot}$ (Woosley 1988).

Also, the late time absolute V light curve of SN 1990K matches that of SN 1987A. The late luminosity of SNe is powered by the γ -rays produced in the radioactive decay of ^{56}Co into ^{56}Fe (half-life = 77.1d). The ^{56}Co is produced by the rapid (half-life = 6.1) radioactive decay of ^{56}Ni generated by nucleosynthesis during the explosion. Because of the slow core expansion velocity, SNe from massive progenitors, like SNII, are expected to be optically thick to γ -rays for a period of about 2 years (Woosley 1988). In fact the luminosity decline rate of SNII up to 2 years after maximum matches very well that expected if all the γ -rays are trapped, i.e. $\gamma = 0.98 \text{ mag } (100d)^{-1}$ (Turatto et al. 1990).

The bolometric luminosity is not available for SN1990K but, since the spectral energy distribution is similar to that of SN 1987A, the V magnitude can be adopted as representative of the bolometric luminosity evolution (Whitelock et al. 1989). The late V decline rate of SN 1990K is consistent with the assumption of complete γ -ray trapping for over 1 year. In this condition the absolute luminosity output at late phase is directly related to the mass of ^{56}Co present at any given moment and, in turn, to the mass of ^{56}Ni synthesized in the explosion. The similar late luminosity of the two SNe indicates that a similar Ni mass ($\sim 0.1 M_{\odot}$) has been produced in both cases. Because, in principle, the amount of Ni produced is a function of the core mass and the mechanism of explosion (Swartz et al. 1991), this suggests a similar core mass for SN 1987 and SN 1990K.

On the other hand, SN 1990K was almost 5 magnitude brighter than SN 1987A at maximum. This can be explained assuming that the progenitor of SN 1990K had an extended radius (3×10^{13} cm), i.e. was a red supergiant, whereas it is known that the faint SN 1987A had a compact progenitor (radius = 3×10^{12} cm). The compact blue supergiant progenitor of SN 1987A has been related to the low metallicity of LMC (Woosley 1988).

The linear early luminosity decline of SN 1990K is possibly related to a small envelope mass. Light curve models indicate that, depending on the presupernova model and explosion mechanism, the envelope mass must be confined in the range $1-5 M_{\odot}$ (Swartz et al. 1991). We found spectroscopic indications that, at late phases, the mass of the envelope of SN 1990K was significantly lower of that SN 1987A. It is therefore concluded that the envelope mass of SN 1990K was 3-5 times smaller than in SN 1987A. We note that since models of SN 1987A adopt an envelope mass of about $10 M_{\odot}$ (Woosley 1988), an envelope mass of 2-3 M_{\odot} seems a reasonable estimate for SN 1990K, in good agreement with the expectation from light curve models.

Because we argued that the ZAMS mass of the two SNe was not very different, the mass loss in the red supergiant phase of the progenitor of SN 1990K should have been quite strong. The detection of this SN at radio wavelengths has not been attempted. We stress that, because of the similarities with the other two SN IIB-L, we would expect SN 1990K to be a radio-loud SN.

5. Conclusion

SN 1990K was a representative of the class of linear SNII, quite similar to SN 1980K. It probably suffered a heavy reddening and, therefore it was very bright at maximum.

The comparison of the observations of this SN with that of other SNII linear and with the reference object SN 1987A suggests that all these SNe come from the same kind of explosion, i.e. core collapse, in similar relatively high-mass, progenitors with different envelope masses and envelope configurations at the time of explosion. A significant constraint is that the mass of ^{56}Ni produced in the explosion should be in all cases close to $0.1 M_{\odot}$.

Acknowledgements. We acknowledge partial financial support from the EC through the Human Capital and Mobility program.

References

- Barbon, R., Ciatti, F., Rosino, L. 1979 A&A 72, 287
 Barbon, R., Ciatti, F., Rosino, L., Ortolani, S., Rafanelli, P. 1982a A&A 116,43
 Barbon, R., Ciatti, F., Rosino, L. 1982b A&A 116, 35
 Barbon, R., Benetti, S., Cappellaro, E., Rosino, L., Turatto, M. 1990 A&A 237, 79.
 Bartunov, O.S. & Blinnikov, S.I. 1992 S.A. Lett 18, 43
 Benetti, S., Cappellaro, E., Turatto, M., Della Valle, M. Gouiffes, C., Mazzali, P. 1993 A&A 285, 147
 Branch, D., Falk, S.W., McCall, M.L., Rybski, P., Uomoto, A.K., Wills, B.J. 1981 ApJ 244,780
 Branch, D., Nomoto, K., Filippenko, A.V. 1991 Comments Astrophys. 15, 221
 Burstein, D. & Heiles, C. Ap.J. 225, 40
 Chugai, N.N., 1988 ApSS 146, 375
 Chugai, N.N., 1991a SvA 17, L400
 Chugai, N.N., 1991b MNRAS 250,513
 Chugai, N.N., 1993 ApJ 414, L101
 Chugai, N.N., & Danziger, I.J. 1994 MNRAS 268, 173
 Cohen, J.G. 1975 Ap.J. 197, 117
 Danziger, J., Lucy, L.B., Bouchet, P., Gouiffes, C. 1991 in *Supernovae* ed. S.E. Woosley, Springer-Verlag, New York p. 69.
 Evans, R. 1990 I.A.U. Circular No. 5022
 Fesen, R.A. & Becker, R.H. 1990 ApJ 351, 437
 Fesen, R.A. & Matonick, D.M. 1993 ApJ 407, 110
 Fransson, C. & Chevalier, R.A. 1987 ApJ 322, L15
 Fransson, C. & Chevalier, R.A. 1989 ApJ 343, 323
 Hanuschik, R.W., Thimm, G., Dachs, J. 1988 MNRAS 234, 41p
 Jeffery, D., Branch, D., 1990, in Wheeler, J.C., Piran, T., Weinberg, S., eds. *Supernovae*, World Scientific Publishing Co., Singapore, p.149.
 Landolt, A.U. 1983 A.J. 88,439
 Landolt, A.U. 1992 A.J. 104,340
 Lucy, L.B., Danziger, I.J., Gouiffes, C. 1991 A&A 243, 223
 Massey, P., Ströbel, K., Barnes, J.V., Anderson, E. 1988 ApJ 328, 315
 Massey, P., Ströbel, K., Barnes, J.V., Anderson, E. 1990 ApJ 358, 344
 Mazzali, P.A., Lucy, L.B., Butler, K. 1992 A&A 258, 399
 McNaught, R.H. & Sadler, E.M. 1990 I.A.U. Circular No. 5024
 Patat, F., Barbon, R., Cappellaro, E., Turatto, M. 1993a A&A Suppl. 98, 443
 Patat, F., Barbon, R., Cappellaro, E., Turatto, M. 1993b A&A 282, 731
 Phillips, M.M. 1990 I.A.U. Circular No. 5027
 Phillips, M.M., Heathcote, S.R. 1989 PASP 101,137
 Phillips, M.M. & Williams, R.E. 1991 in *Supernovae* ed. S.E. Woosley, Springer-Verlag, New York p. 36.
 Schmidt, B.P. et al. 1993 AJ 105, 2236
 Spyromilio, J., Meikle, W.P.S., Allen, D.A. 1990 MNRAS 242,669
 Spyromilio, J., Stathakis, R.A., Cannon, R.D. 1991 in *SN 1987A and other Supernovae* eds. I.J.Danziger & K. Kjär ESO Workshop and Conference Proceedings No. 37, p. 225
 Swartz, D.A., Wheeler, J.C., Harkness, R.P. 1991 ApJ 374,266
 Stone, R.P.S. 1977 ApJ 218, 767
 Stone, R.P.S. & Baldwin, J.A. 1983 MNRAS 204, 347
 Stone, R.P.S. & Baldwin, J.A. 1984 MNRAS 206, 241
 Turatto, M., Cappellaro, E., Barbon, R., Della Valle, M., Ortolani, S., Rosino, L. 1990 AJ 100, 771
 Turatto, M., Cappellaro, E., Benetti, S., Danziger, J. 1993 MNRAS 265, 471
 Tully, R.B. 1988 *Nearby galaxies catalog* Cambridge University Press (Cambridge)
 Uomoto, A. & Kirshner, R.P. 1986 ApJ 308, 685
 Weiler, K.W., Sramek, R.A., Panagia, N. 1991a in *SN 1987A and other Supernovae* eds. I.J.Danziger & K. Kjär ESO Workshop and Conference Proceedings No. 37, p. 633
 Weiler, K.W., Van Dyk, S.D., Panagia, N., Sramek, R.A., Discenna, J.L. 1991b ApJ 380,161
 Weiler, K.W., Van Dyk, S.D., Panagia, N., Sramek, R.A., 1992 ApJ 398,248
 Whitelock, R.M. et al. 1989 MNRAS 240, 7p
 Williams, R.E. 1987 ApJ 320, L117
 Witteborn, F.C., Bregman, J.D., Wooden, D.H., Pinto, P.A., Rank, D.M., Woosley, S.E. 1989 p.J. 338, L9
 Woosley, S.E. 1988 ApJ 330, 218
 Young, T.R., & Branch, D. 1989 ApJ 342, L55

This article was processed by the author using Springer-Verlag L^AT_EX A&A style file version 3.